Cell Reports

Article

Roof Plate-Derived Radial Glial-like Cells Support Developmental Growth of Rapidly Adapting Mechanoreceptor Ascending Axons

Graphical Abstract

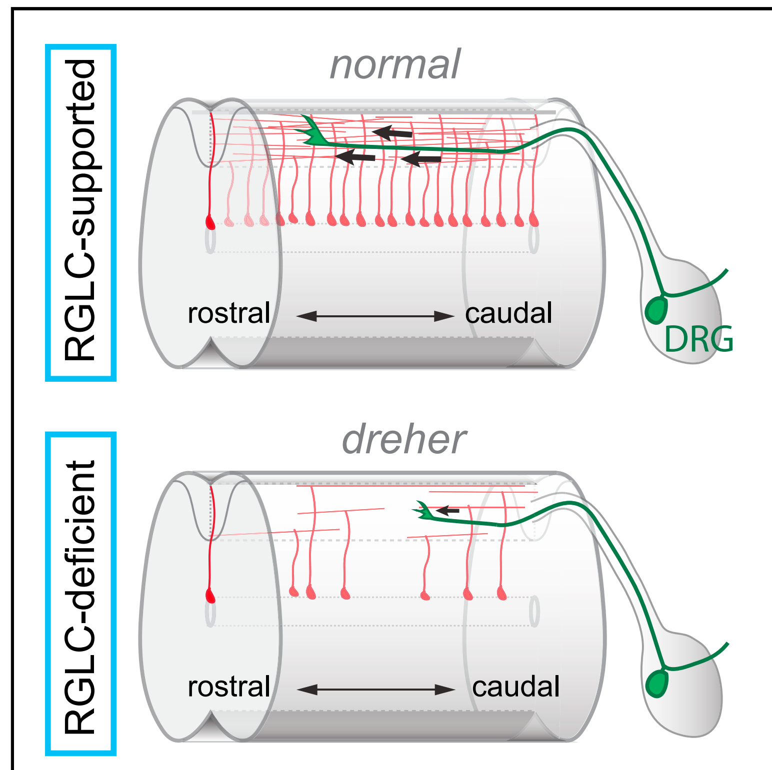

Highlights

- Radial glial-like cells (RGLCs) exist in the developing dorsal column midline
- RGLCs are derived from the roof plate
- RGLCs form a scaffold of processes, which express growth-supportive factors
- RGLCs are required for growth of long-range dorsal column axons

Authors

Kim Kridsada, Jingwen Niu, Parthiv Haldipur, ..., Victor V. Chizhikov, Kathleen J. Millen, Wenqin Luo

Correspondence

kathleen.millen@seattlechildren.org (K.J.M.),
luow@pennmedicine.upenn.edu (W.L.)

In Brief

Kridsada et al. identified a population of roof plate-derived radial glial-like cells in the dorsal midline of the developing spinal cord. These cells form a growth-supportive “highway” for developing long-projecting spinal cord axons. This study provides direct evidence for a glia-axon developmental growth mechanism.

Data and Software Availability

GSE114193

Kridsada et al., 2018, Cell Reports *23*, 2928–2941
June 5, 2018 © 2018 The Authors.
https://doi.org/10.1016/j.celrep.2018.05.025

CellPress

OPEN ACCESS
CellPress

Cell Reports
Article

Roof Plate-Derived Radial Glial-like Cells Support Developmental Growth of Rapidly Adapting Mechanoreceptor Ascending Axons

Kim Kridsada,[1,9] Jingwen Niu,[1,7,9] Parthiv Haldipur,[2] Zhiping Wang,[3] Long Ding,[1] Jian J. Li,[4] Anne G. Lindgren,[5] Eloisa Herrera,[6] Gareth M. Thomas,[7] Victor V. Chizhikov,[8] Kathleen J. Millen,[2,*] and Wenqin Luo[1,10,*]
[1]Department of Neuroscience, University of Pennsylvania, Philadelphia, PA 19104, USA
[2]Seattle Children's Hospital Research Institute, Center for Integrative Brain Research, Seattle, WA 98105, USA
[3]Department of Biostatistics, University of Pennsylvania, Philadelphia, PA 19104, USA
[4]Department of Neurology, University of Pennsylvania, Philadelphia, PA 19104, USA
[5]STAAR Surgical, Monrovia, CA 91016, USA
[6]Instituto de Neurociencias de Alicante (Consejo Superior de Investigaciones Científicas-Universidad Miguel Hernández, CSIC-UMH), Campus San Juan, Av. Ramón y Cajal s/n, Alicante 03550, Spain
[7]Shriners Hospital's Pediatric Research Center (Center for Neurorehabilitation and Neural Repair), Lewis Katz School of Medicine, Temple University, 3500 N. Broad Street, Philadelphia, PA 19140, USA
[8]Department of Anatomy and Neurobiology, Health Science Center, University of Tennessee, Memphis, TN 38163, USA
[9]These authors contributed equally
[10]Lead Contact
*Correspondence: kathleen.millen@seattlechildren.org (K.J.M.), luow@pennmedicine.upenn.edu (W.L.)
https://doi.org/10.1016/j.celrep.2018.05.025

SUMMARY

Spinal cord longitudinal axons comprise some of the longest axons in our body. However, mechanisms that drive this extra long-distance axonal growth are largely unclear. We found that ascending axons of rapidly adapting (RA) mechanoreceptors closely abut a previously undescribed population of roof plate-derived radial glial-like cells (RGLCs) in the spinal cord dorsal column, which form a network of processes enriched with growth-promoting factors. In *dreher* mutant mice that lack RGLCs, the lengths of ascending RA mechanoreceptor axon branches are specifically reduced, whereas their descending and collateral branches, and other dorsal column and sensory pathways, are largely unaffected. Because the number and intrinsic growth ability of RA mechanoreceptors are normal in *dreher* mice, our data suggest that RGLCs provide critical non-cell autonomous growth support for the ascending axons of RA mechanoreceptors. Together, our work identifies a developmental mechanism specifically required for long-range spinal cord longitudinal axons.

INTRODUCTION

The spinal cord bridges the periphery and brain through ascending pathways that convey sensory input and descending pathways that control motor output. During development of the vertebrate nervous system, these longitudinal axons project over considerable distances and, in some cases, span nearly the entire length of the spinal cord. After development, however, these axons rarely regenerate upon spinal cord injury or axon degeneration, leading to serious sensory and motor dysfunction. At present, there has been little success in promoting regrowth of mammalian spinal cord longitudinal axons. Therefore, understanding the mechanisms underlying longitudinal axon growth during development is critical, with the hope of ultimately developing better therapeutic strategies for promoting axon regeneration after spinal cord injury.

Morphogen signaling gradients have previously been shown to play an important role for the pathfinding along the anterior-posterior axis of the spinal cord and local growth of several types of spinal cord axons during development. In mice, post-commissural axons are guided rostrally through Fz3-mediated attraction to a rostral Wnt4 gradient (Lyuksyutova et al., 2003) and repulsion from a caudal Shh gradient (Yam et al., 2012). In chick, this turning is attributed to a rostral Wnt5a/7a chemoattractant activity gradient, as well as a Hip-mediated chemorepulsive Shh gradient (Bourikas et al., 2005). Moreover, a descending Wnt gradient in the mouse dorsal spinal cord has been proposed to repel corticospinal tract (CST) axons in their descent during development (Liu et al., 2005). These studies highlight the axon guidance function and local growth support of morphogen gradients, but less work has specifically examined the development mechanisms underlying axon growth support across long distances, particularly for axons that must span the entire spinal cord.

One of these major long-distance projecting axon bundles in the spinal cord is the mammalian dorsal column funiculus. The dorsal column contains two ipsilaterally ascending pathways, the direct dorsal column (DDC) and post-synaptic dorsal column (PSDC) pathways, which comprise the axons of primary somatosensory dorsal root ganglion (DRG) neurons and dorsal horn spinal cord neurons, respectively (Figure 1A). These two ascending pathways transmit light touch, body position, and

 © 2018 The Authors.
This is an open access article under the CC BY-NC-ND license (http://creativecommons.org/licenses/by-nc-nd/4.0/).

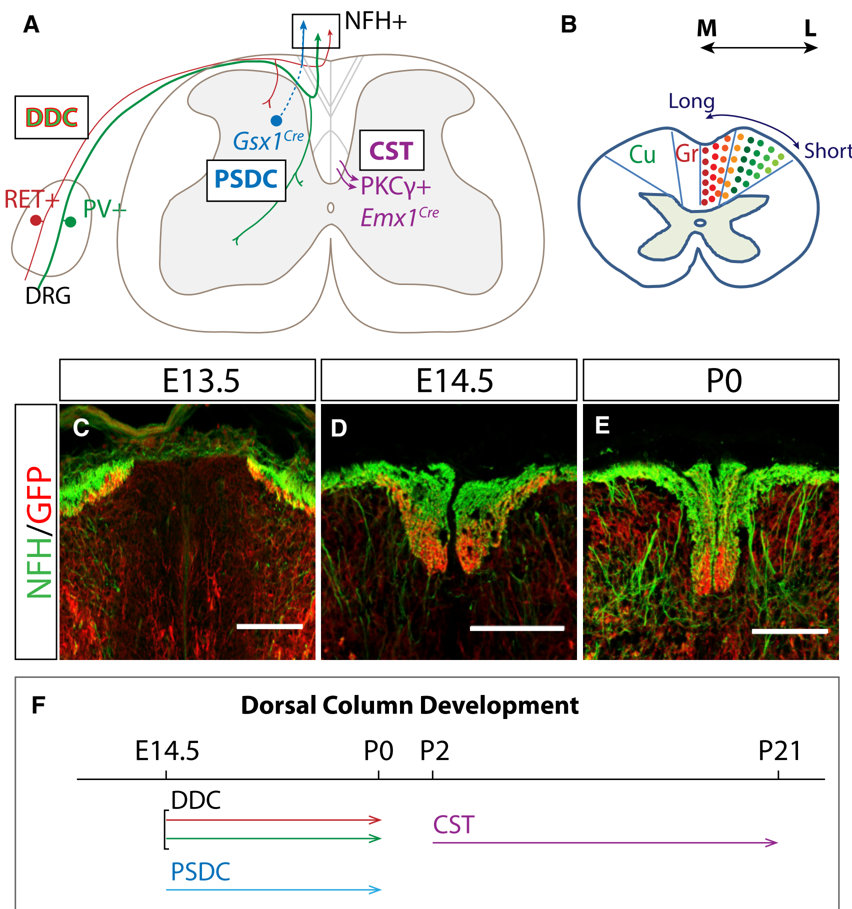

Figure 1. Development of the Dorsal Column Pathways in the Spinal Cord

(A) Schematic representation of ascending (left) and descending (right) pathways in the dorsal column and the corresponding molecular markers or genetic tracing strategies used in this study (RET^+ mechanoreceptors and PV^+ proprioceptors comprise DDC pathway, NFH labels both DDC axons, $Gsx1^{Cre}$ labels the PSDC pathway, and the CST is labeled by $Emx1^{Cre}$ and PKCγ).

(B) Functional organization of the two main DDC axon types in a dorsal column cross-section at the cervical level along the medial (M) to lateral (L) axis (mechanoreceptive, red; proprioceptive, green; Gr, gracile fasciculus; Cu, cuneate fasciculus).

(C–E) Co-staining of $Gsx1^{Cre}$; Tau^{mGFP} embryonic thoracic spinal cord in transverse plane with NFH and GFP at E13.5 (C), E14.5 (D), and P0 (E) to label DDC and PSDC axons, respectively. Scale bar, 100 μm. n = 3 mice.

(F) A schematic frame showing the developmental time window of different dorsal column pathways.

other somatosensory information to the brain stem. In the rodent spinal cord, the corticospinal tract (CST) also descends in the most ventral part of the dorsal column (Figure 1A).

We previously characterized the functional organization of the DDC pathway (Niu et al., 2013), which contains the ascending axons of Aβ mechanoreceptors and proprioceptors. We showed that ascending axons of Aβ rapidly adapting (RA) mechanoreceptors and proprioceptors are largely segregated. RA mechanoreceptive axons, which span the entire length of the spinal cord and innervate the medulla, ascend medially. In contrast, proprioceptive axons, which only span a few spinal cord segments, ascend laterally. Furthermore, a somatotopic organization exists within each modality, with the most caudal-originating axons projecting closest to the midline. As a result, the longest dorsal column axons are closest to the dorsal midline (Figure 1B). This functional organization suggests that some mechanism takes place at the midline to promote/maintain extra long-distance axonal growth so that ascending axons of caudal RA mechanoreceptors can reach their distant targets in the brain.

Here, we show that during development the roof plate of the spinal cord gives rise to a population of radial glial-like cells (RGLCs) in the dorsal column midline. These RGLCs are enriched for axon growth-promoting factors and form a network of processes that closely appose the growing ascending axons of RA mechanoreceptors during development. Our RNA sequencing analysis identified several growth-promoting factors expressed by RGLCs, suggesting a potential mechanism by which growth support is sustained throughout the spinal cord. Interestingly, *dreher* mutant mice, which lack RGLCs, display a specific impairment in the long-distance projecting ascending axon branches of caudal RA mechanoreceptors, while their descending axon branches and spinal cord -innervating collaterals, as well as other types of dorsal column and sensory axons, are unaffected. Moreover, the number and intrinsic growth ability of RA mechanoreceptors are normal in *dreher* mutants. Taken together, our results reveal an important cellular mechanism in which roof plate-derived RGLCs form a scaffold and potential source of growth factors that support and/or maintain extra long-distance growth of spinal cord longitudinal axons.

RESULTS

Development of Ascending and Descending Dorsal Column Pathways

To investigate the possible mechanisms underlying the long-distance trajectories of dorsal column axons in the spinal cord, we first characterized the normal developmental process of the dorsal column funiculus. To visualize the dorsal column pathways, we performed immunohistochemistry in $Gsx1^{Cre}$; Tau^{mGFP} mice for neurofilament heavy chain (NFH), which labels DDC axons. The $Gsx1^{Cre}$ allele (Cui et al., 2016) allowed us to genetically label most dorsal spinal cord neurons, including PSDC neurons, with a neuron-specific Tau^{mGFP} reporter allele by inducing expression of myristoylated green fluorescent protein (mGFP) upon Cre recombination. Around E13.5, the DDC and PSDC axons reached the dorsal spinal cord but paused lateral to the presumptive dorsal column region (Figure 1C). They started to

form the dorsal column at E14.5 (Figure 1D). By P0, the dorsal column was fully formed (Figure 1E), at which point the DDC fibers have completed their ascent to their final targets in the dorsal column nuclei (Wessels et al., 1991). We observed a clear segregation between the dorsally positioned DDC axons and the ventrally positioned PSDC axons in the dorsal column throughout development (Figures 1C–1E), which was consistent with a previous study using a different mouse line, *EphA4*^{AP}, to label PSDC axons (Paixão et al., 2013). This ventral dorsal column localization of PSDC axons was also shown by a previous study using *EphA4*^{AP} mice. Next, we used *Emx1*^{Cre}*; Tau*^{mGFP} mice to genetically trace CST descending axons. In agreement with previous reports (Liu et al., 2005), we found that the CST developed postnatally, descending around P1 and reaching the lumbar level around P7 (Figures S1A–S1D″). Altogether, our results reveal that the ascending (DDC and PSDC) and descending (CST) dorsal column pathways develop in non-overlapping time windows (Figure 1F), suggesting their developmental growth is likely mediated by distinct mechanisms.

RNA Sequencing of Isolated Dorsal Midline Cells and RA Mechanoreceptors

From our developmental analyses, we noticed a visible separation maintained between the left and right sides of the primitive dorsal column throughout development (Figures 1C–1E). To gain further insight into the midline composition, we performed H&E staining and found a number of nuclei residing in the dorsal column midline at E14.5. To reveal the identity of the dorsal midline cells and uncover possible molecular midline cell-axon interactions, we isolated dorsal column midline cells at E14.5 using hematoxylin staining and laser capture microdissection (LCM) (Figure 2A). For transcript comparison, RA mechanoreceptors were genetically labeled using a *Ret*^{CreERT2}*; Rosa*^{Tdt} mouse (Ret-Tdt) (Fleming et al., 2015; Luo et al., 2009) and purified by fluorescently activated cell sorting (FACS) of the DRG (Figure 2B). Principal component analysis (PCA) of relative fold change across all samples revealed two distinct clusters, which comprised the three biological replicates of LCM cells and RA mechanoreceptors, respectively (Figure 2C). Hierarchical clustering of relative gene expression between LCM cells and RA mechanoreceptors also confirmed distinct segregated patterns between the two cell types, revealing large groups of transcripts specifically enriched in each population (Figure 2D). Profile comparisons through volcano plot analysis showed a large distribution of genes with over 5-fold differential expression between LCM and Ret-Tdt replicates (false discovery rate [FDR] < 0.05) (Figure 2E). Notably, relative transcript levels of known markers specific for neurons and RA mechanoreceptors (such as *Gfra2*, *Ret*, *P2rx3*) were highly enriched in Ret-Tdt replicates, while radial glial cell-specific markers (such as *Pax6*, *Sox2*, *Gli3*, *Nestin*) were enriched in LCM replicates (Figure 2F). Through Kyoto Encyclopedia of Genes and Genomes (KEGG) analysis, we identified multiple molecular pathways enriched in the dorsal midline cells (Figures S1E and S1F), some of which are highly related to axon growth, including extracellular matrix (ECM)-receptor interactions, axon guidance and adhesion molecules, and growth factors.

To show that some of these growth factors can function in promoting RA mechanoreceptor axon growth, we ranked the normalized read counts of the LCM transcripts, and identified the top surface-expressed or secreted growth factors (Figure S2A). With these criteria, three candidate growth factor genes—insulin-like growth factor 1 (*Igf1*), insulin-like growth factor 2 (*Igf2*), and pleiotrophin (*Ptn*)—were selected and their expression at the dorsal column midline were validated with *in situ* hybridization at E14.5 (Figures S2B–S2E′). We then cultured dissociated DRG from E16 rat embryos, a developmental stage equivalent to E14.5 mouse embryos, and supplemented media with neurturin (NRTN), the ligand for the RET receptor expressed in RA mechanoreceptors (Luo et al., 2009), to specifically enrich this population of DRG neurons, and then added the growth factors individually or in combination (Figure S3). We found that IGF1, but not IGF2 or PTN, robustly increased axonal growth of RA mechanoreceptors (Figure S3F). Our results suggest that the dorsal column midline cells could support axon growth of RA mechanoreceptors through secreted growth factors.

Dorsal Midline Cells Originate from the Roof Plate

The RNA sequencing analyses identified a number of molecular markers for the dorsal column midline cells. Among these markers, the transcription factor ZIC2 strongly labeled nuclei of the dorsal column midline cells, in addition to some dorsal spinal cord neurons (Escalante et al., 2013), during the dorsal column developmental time window (Figures 3A–3B′). At E13.5, ZIC2^{+} cells occupied the medial dorsal area between each side of the DDC and PSDC axon fascicles throughout the spinal cord (Figures 3A and 3A′). Around E14.5, the ZIC2^{+} cells began to elongate, migrating ventrally toward the central canal (Figures 3B and 3B′) to form a thin septum between the left and right sides of the dorsal spinal cord around E15.5 (Figures 3D and 3D′). By P0, ZIC2 was no longer strongly detected at the dorsal midline (Figures 3C and 3C′), suggesting that the midline cells either disappeared or downregulated ZIC2 by the time the ascending dorsal column axons arrived at the dorsal column nuclei. In line with the RNA sequencing results, we also confirmed *Nestin* expression, a radial glial progenitor marker, by *in situ* hybridization (Figures S2E and S2E′) and immunostaining in dorsal midline cells by E14.5 and E15.5 (Figures 3E and 3E′), and BLBP, a glia-specific marker (Figure 3F and 3F′). Postnatally, NESTIN, BLBP, as well as NCAM were robustly detected at the dorsal column midline as well (Figures 3G and S2F). These results further support the radial glial identity of the dorsal column midline cells.

Next, we sought to examine the developmental origin of the midline cells. Because ZIC2 and NESTIN are both expressed in meningeal cells (Figures 3A–3E), we first determined whether the midline cells were derived from the meninges with immunostaining. While PGD2 synthase, a meningeal cell-specific marker, was expressed in the meninges as expected, it was not expressed by the ZIC2^{+} dorsal column midline cells (Figures 3D–3D′), suggesting that dorsal column midline cells are not derived from the meninges.

Given the importance and anatomical position of the roof plate during development, we next tested the possibility whether the ZIC2^{+} dorsal midline cells might be derived from the roof plate. Using a roof plate-specific Cre transgenic mouse line, *Lmx1a*^{Cre} (Chizhikov et al., 2010), we genetically labeled roof plate-lineage

OPEN ACCESS
CellPress

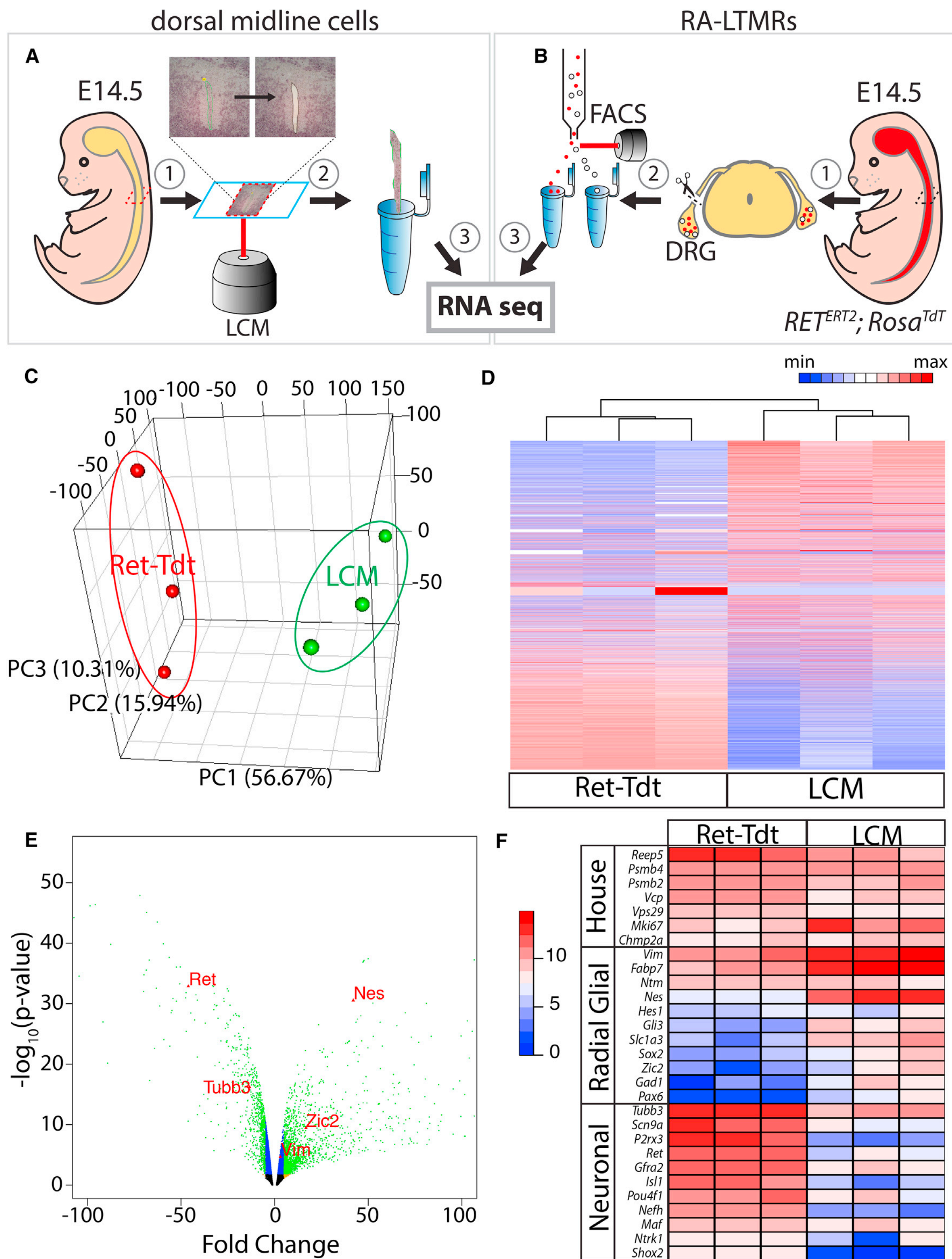

Figure 2. RNA Sequencing of Isolated Dorsal Midline Cells and RA Mechanoreceptors Reveal Radial Glial and Neuronal-Specific Marker Expression

(A and B) Isolation and purification of dorsal column midline cells by LCM (A) and RA mechanoreceptors by genetically labeling (*Ret*^{CreERT2}; *Rosa*^{Tdt} line [Ret-Tdt]) and FACS (B) from E14.5 embryos for RNA sequencing. n = 3 mice for each group.

(C) Principal component analysis (PCA) of transcripts collected from each embryo assigned LCM and mechanoreceptors (Ret-Tdt) replicates to two distinct clusters (indicated by green and red ovals).

(legend continued on next page)

OPEN
ACCESS
CellPress

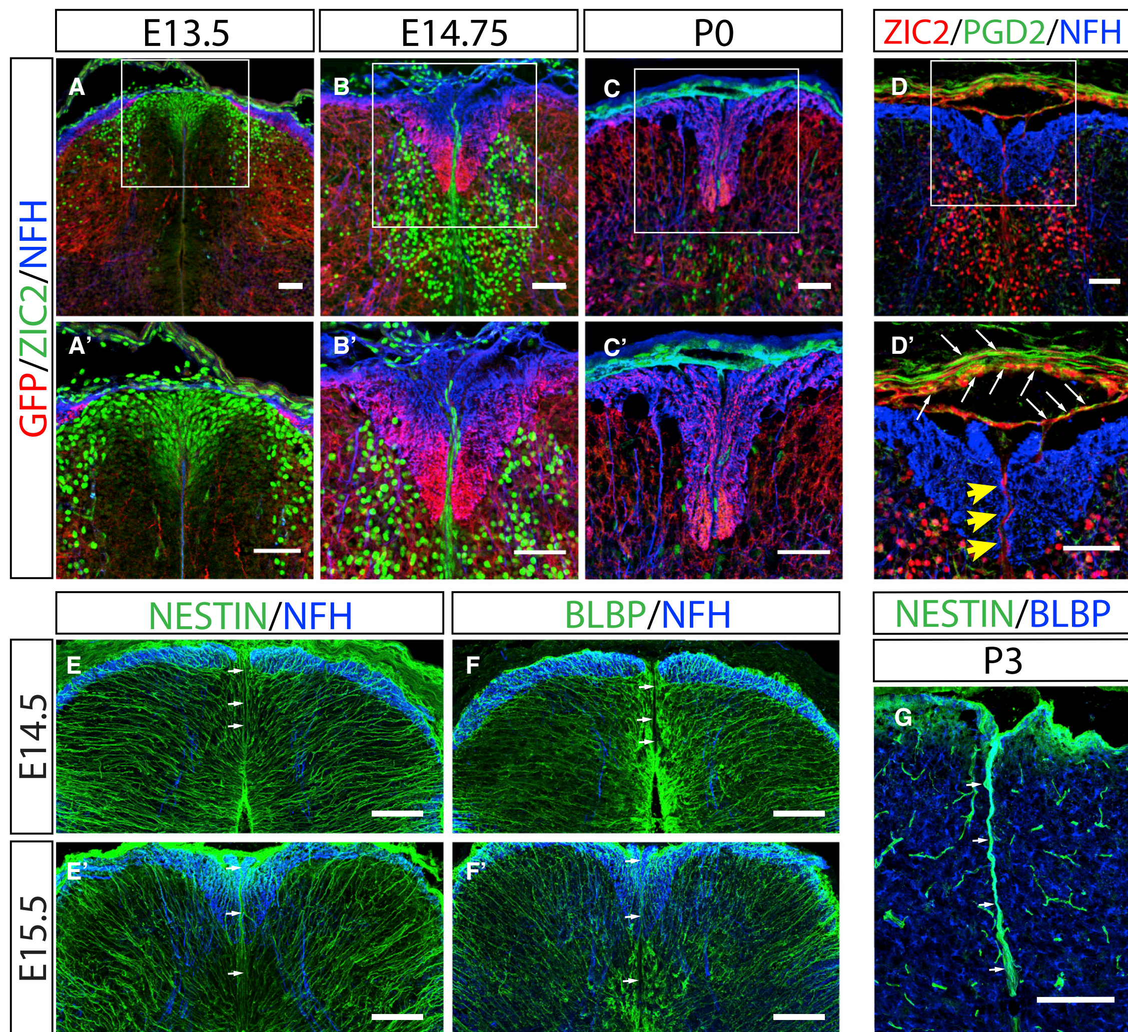

Figure 3. Dorsal Midline Cells Express ZIC2 and Radial Glial Markers

(A–C′) Co-staining of *Gsx1*^{cre}*; Tau*^{mGFP} thoracic spinal cord using antibodies against GFP, ZIC2, and NFH to reveal PSDC axons, dorsal midline cells, and DDC axons, respectively, in the dorsal column at different developmental stages E13.5 (A and A'), E14.75 (B and B'), and P0 (C and C'). High power images boxed in (A)–(C) are shown in (A′)–(C′).

(D and D′) Co-staining of an E15.5 lumbar dorsal column with antibodies against ZIC2, PGD2 (prostaglandin D2 synthase), and NFH. PGD2 marks the meningeal cells in pia mater, some of which co-express ZIC2 (white arrows), but not dorsal column midline cells (yellow arrowheads).

(E–G) Staining of thoracic (E–F′) and lumbar (G) spinal cord using an antibody for radial glial marker progenitor NESTIN and glial-specific marker BLBP at E14.5 (E and E′), E15.5 (F and F′), and P3 (G). White arrows indicate dorsal column midline.

Scale bars, 100 μm (A–J and E′–F′), 50 μm (A′–D′). n = 3 mice for each.

cells with a *Rosa26*^{Tdt} reporter line. We found that Tdt-labeled roof plate cells co-localized with ZIC2 expression in the dorsal medial spinal cord at E13.5 (Figures 4A and 4A′). Although ZIC2 expression was later downregulated at E16.5 and E17.5, the Tdt^{+} cells continued to reside in the dorsal midline throughout the remaining embryonic and postnatal development (Figures 4B–4C′ and S2H–S2I′), providing a separation between the left and right dorsal column axons (Figures 4D and 4D′). Furthermore, the roof plate-lineage midline cells do not express meningeal marker ZO-1 (Figure S2G) but do express radial glial

(D) Hierarchical clustering of transcript fold changes of LCM replicates compared to Ret-Tdt replicates.

(E) Differential volcano plot analysis of LCM versus Ret-Tdt transcriptomes, with Ret-Tdt differentially enriched genes indicated by negative fold changes (FC) and LCM differentially enriched genes indicated by positive FCs. Green dots represent genes differentially expressed with absolute value FC above 10. FC cutoff = ±5. Markers enriched in RA mechanoreceptors (Ret, Tubb3) or LCM cells (Nes, Vim, Zic2) are highlighted.

(F) Heatmap distribution of neuronal and radial glial cell-specific markers based on absolute normalized transcripts from Ret-Tdt and LCM transcriptomes. Housekeeping genes presented for comparison.

OPEN ACCESS
CellPress

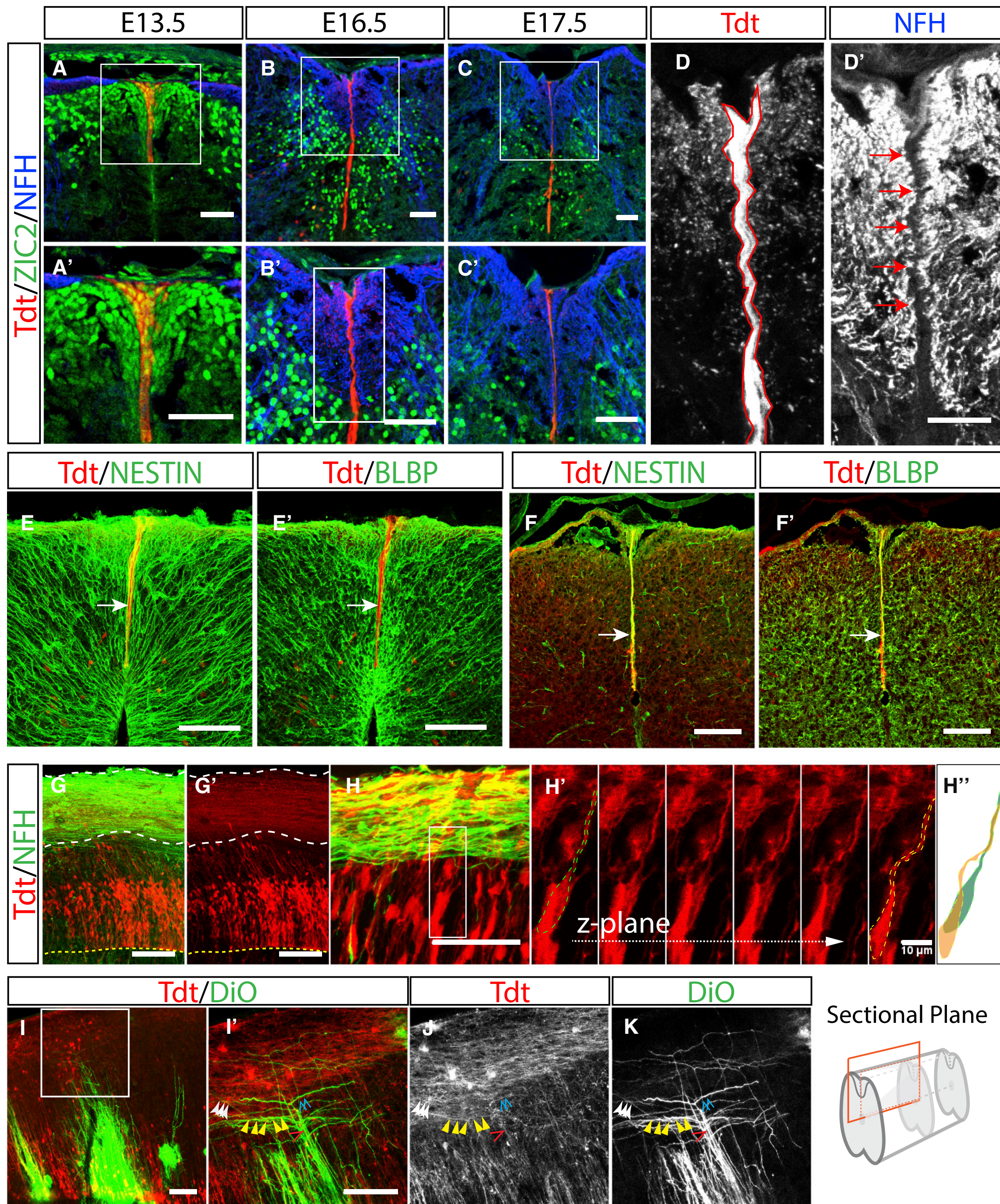

Figure 4. Dorsal Column Midline Cells Are Derived from the Roof Plate and Display Radial Glial Cell Morphology

(A–C′) Co-staining of embryonic *Lmx1a*^{Cre}*; Rosa26*^{Tdt} thoracic (A and A′) and lumbar (B–D′) spinal cord dorsal column with Tdt, ZIC2 and NFH to show roof plate-derived cells, dorsal midline cells and DDC axons, respectively, at E13.5 (A and A′), E16.5 (B and B′), and E17.5 (C and C′). (A′–C′) are higher magnifications of boxed regions in (A–C).

(D and D′) High magnification of boxed area in (B′) with Tdt (D) and NFH (D′) in separated channels. Red arrows indicate the midline gap (filled with Tdt^{+} midline cells) separating left and right sides of the dorsal column axons (NFH^{+}).

(E–F′) Staining of *Lmx1a*^{Cre}*; Rosa26*^{Tdt} cervical (E and E′) and lumbar (F and F′) dorsal column with NESTIN and BLBP at E14.5 (E and E′) and P3 (F and F′). White arrows indicate dorsal column midline.

(G–H″) Co-staining of longitudinal *Lmx1a*^{Cre}*; Rosa26*^{Tdt} thoracic spinal cord sections at E14.5 (H and H′) and E15.5 (G and G′) with Tdt and NFH. See orange rectangle in schematic below for longitudinal sectional plane. In (G and G′), longitudinal dorsal column fibers are delineated by white dotted lines, and the central

(legend continued on next page)

OPEN
ACCESS
CellPress

markers NESTIN (Figure 4E and 4F) and BLBP (Figures 4E′ and 4F′) as early as E14.5.

To gain additional insight into midline cell morphologies, we examined longitudinal spinal cord sections along the spinal cord midline. During dorsal column development, the somas of the roof plate-derived cells descended from the dorsal midline toward the central canal. The midline cells developed a bipolar morphology, with a basal process anchored in the central canal and apical processes attached to the pia (Figures 4G and 4G′). Single cell reconstruction at E14.5 revealed that the Tdt$^+$ cells exhibited classic radial glial morphology at this stage (Figures 4H–4H″). By E15.5, their radial processes were fully extended. At P3, we sparsely labeled the Tdt$^+$ cells with a small amount of DiO to reveal morphologies of individual cells. The DiO$^+$/Tdt$^+$ apical processes branched and formed a network running parallel to the dorsal column axons, in close apposition with the two sides of the dorsal column fascicle (Figures 4I–4K). These midline cells persisted at the dorsal column midline at 3 weeks, at which point they appeared to become quiescent, ependymal-like cells lining the central canal (Figures S2H–S2I′). Collectively, our results reveal that these dorsal column midline cells are derived from roof plate cells to form a septum that separates the left and right dorsal spinal cord. These cells retain both morphological and molecular traits of radial glia, so we hereafter call them dorsal column radial glial-like cells (RGLCs).

Roof Plate-Deficient *Dreher* Mice Fail to Generate RGLCs

The close proximity of RGLCs to developing DDC and PSDC ascending axons and their expression of a variety of growth factors and axon guidance molecules during development made them attractive candidates for supporting the long-distance growth of dorsal column axons. To test this hypothesis, we utilized mouse lines carrying *dreher* (*dr*) alleles that harbor spontaneous null mutations of the *Lmx1a* gene (Bergstrom et al., 1999), either through point mutation (dr^J) or deletion (dr^{6J}) (Chizhikov et al., 2006; Millonig et al., 2000). Subsequently, these mice display deficits with cells derived from the roof plate (Millonig et al., 2000). One of these alleles, the dr^{6J} allele, is known to carry a loss-of-function deletion of the *Lmx1a* gene spanning exons 4 through 8 (Figure S4A). Our mapping revealed that the deletion segment started ~2,250 bp upstream of exon 4 and ended ~3,930 bp downstream of exon 8 of the *Lmx1a* gene, without disrupting other flanking genes (Figures S4B and S4C). This result indicates that the dr^{6J} allele is a pure null mutation for *Lmx1a*.

To verify that the RGLCs were absent in the *dreher* mutant mice, we stained for ZIC2, NESTIN, and BLBP, which we established as markers for the RGLCs. Not only were the number of ZIC2$^+$ midline cells greatly reduced in the dr^{6J}/dr^{6J} mutant dorsal column (Figures 5A and 5B), but all radial glial markers were completely absent in the dorsal column midline when compared to controls (Figures 5C and 5D). Because the absence of marker expression could be caused by either a loss of the midline cells or changes of gene expression, we genetically labeled RGLCs in *dreher* mutant mice using $Lmx1a^{Cre}$ with a LacZ reporter and the dr^J mutant allele. The $Lmx1a^{Cre}$ BAC transgene was fused with GFP, which was detectable using a GFP antibody (Figures 5E and 5F, white arrow heads). In wild-type embryonic spinal cord, we observed LacZ-labeled *Lmx1a*-lineage cells in the dorsal midline, neural crest-lineage cells (including the DRG), and scattered dorsal interneurons within the spinal cord (Figures 5G and 5I). In dr^J/dr^J mutant spinal cord, we saw specific deletion of the LacZ$^+$ dorsal midline cells, despite grossly normal positioning of LacZ$^+$ *Lmx1a*-lineage dorsal spinal cord interneurons (Figures 5H and 5J). The same was true for postnatal stages examined at P7 and P21 (Figures 5K–5N). Quantification of LacZ$^+$ cells in the ependymal layer of the central canal at P21 (Figures 5M′–5N′) revealed no LacZ-labeled cells in the mutants (Figure 5O). Taken together, we concluded that RGLCs are absent in the *dreher* mice, and we subsequently used these animals as a model to examine RGLC-deficient conditions *in vivo*.

Dorsal Spinal Cord Integrity Is Grossly Preserved in *Dreher* Mutant Mice

The roof plate plays a substantive role during early development to dorsalize the neural tissue and generate dI1 interneurons (Augsburger et al., 1999; Lee et al., 2000; Liem et al., 1997; Millen et al., 2004). One concern with *dreher* mutant mice is whether dorsal spinal cord interneurons are massively altered in the absence of a functional roof plate. A recent study used genetic tracing to show that mature dI1 neurons reside in the intermediate spinal cord (Yuengert et al., 2015). Our own genetic tracing of *Lmx1a*-lineage cells revealed a population of labeled interneurons in the same region of the control and dr^J/dr^J spinal cord (Figures 5E–5N, open arrows), suggesting that at least some dI1 neurons are generated and migrate to their mature locations in the *dreher* mutant mice. Interestingly, other early born dorsal populations such as dI2 (marked by Lhx1/5$^+$/Pax2$^-$) and dI3 (marked by Isl1$^+$) (Helms and Johnson, 2003), and late-born dorsal populations dILA and dILB neurons, which respectively express Pax2$^+$ and Lmx1b$^+$ (Mizuguchi et al., 2006), are generated in normal numbers in dr^J/dr^J mutant mice (Figures S5A–S5H, S5S, and S5T). Together, these data demonstrate that many dorsal spinal interneurons are still generated and develop in the absence of *Lmx1a*.

To further demonstrate that the distribution of mature spinal cord interneuron types is roughly normal in *dreher* mutants, we performed *in situ* hybridization with RNA probes for excitatory (*Vglut2*) and inhibitory (*Glyt2*, *Gad1/2*, *Vgat*) neuronal markers

canal is indicated by the yellow dotted line. (H′) is high magnification of boxed area in (H). (HV′) Inset is high magnifications of boxed region in (H), projected along the z plane. Single Tdt$^+$ cells are outlined in dotted yellow and green dotted lines. (H″) is a representation of the two cells outlined in (H′).

(I–K) DiO injection targeting Tdt$^+$ cell bodies from longitudinal $Lmx1a^{Cre}$; $Rosa26^{Tdt}$ thoracic spinal cord sections at P3 to show cell morphology of roof plate-derived cells (I). High power image boxed in (I) are shown in (I′), with separated channels in (J and K). Color-coded arrowheads denote individual processes (shared colors indicate the same branch) and colocalization of Tdt$^+$ and DiO labeling.

Scale bars, 100 μm (A′–C′, D–E′, G, and G′), 150 μm (F and F′), 50 μm (A–C and H), and10 μm (H′). n = 3 mice for each.

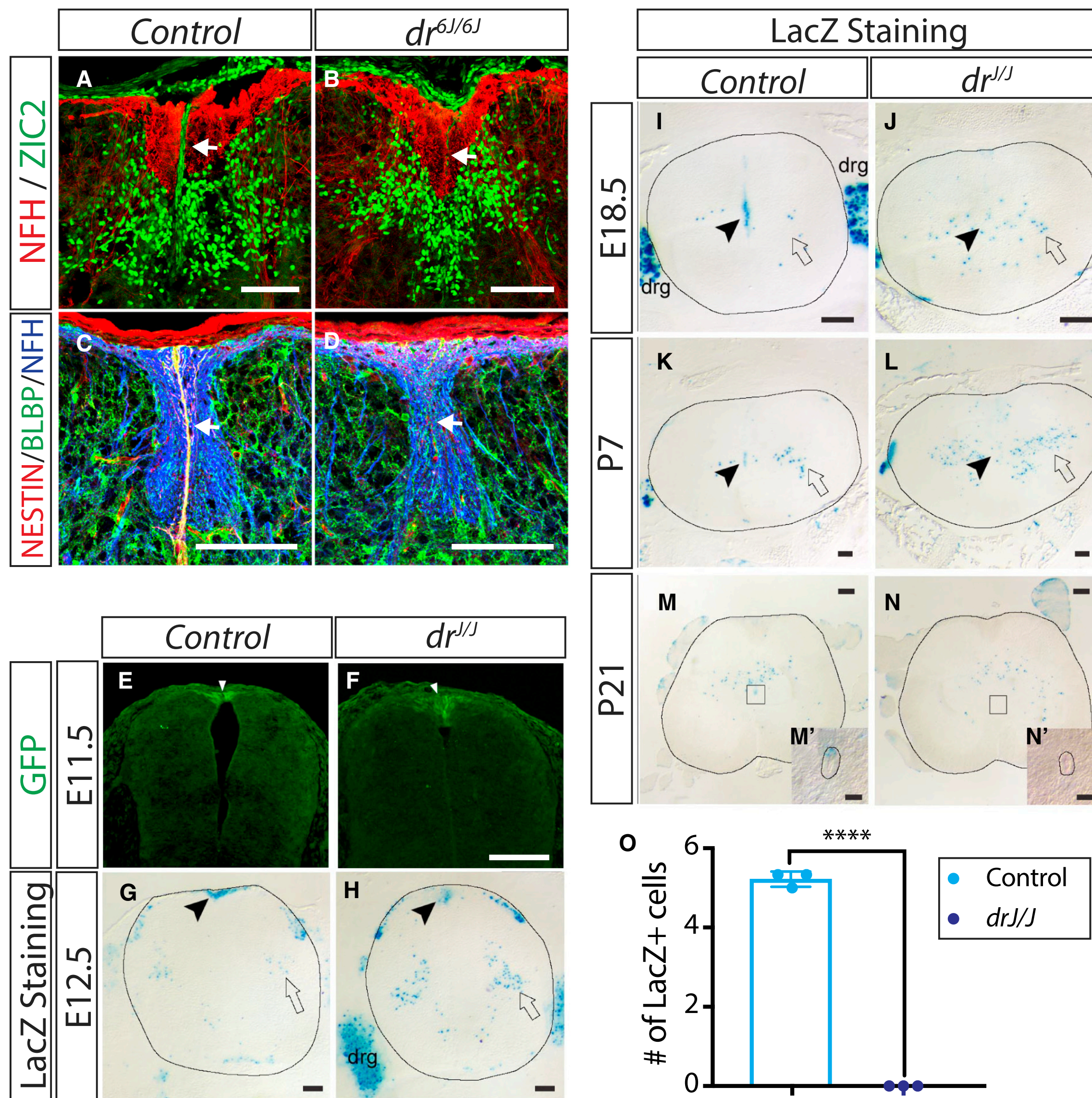

Figure 5. Roof Plate-Deficient *dreher* Mutants Fail to Generate Dorsal Column Midline Cells

(A and B) Co-staining of E15.5 control (A) and dr^{6J}/dr^{6J} mutants (B) thoracic spinal cord sections with antibodies against ZIC2 and NFH. White arrows indicate ZIC2^{+} RGLCs.

(C and D) Co-staining of P0 control (C) and dr^{6J}/dr^{6J} mutants (D) spinal cord sections with radial glial makers BLBP and NESTIN with NFH. White arrows indicate BLBP^{+}/NESTIN^{+} RGLCs.

(E and F) Lineage tracing of *Lmx1a* expression through *Lmx1a*^{Cre} transgene fused with GFP in control (E) and dr^{J}/dr^{J} (F) mutant e11.5 spinal cord, detected by immunohistochemistry for GFP. Arrowheads indicate GFP^{+} cells in roof plate region.

(G–N) Lineage tracing of *Lmx1a* expressing roof plate cells using *Lmx1a*-LacZ staining in control and dr^{J}/dr^{J} mutant spinal cords at E12.5 (G and H), E18.5 (I and J), P7 (K and L), and P21 (M and N). Filled arrowheads indicate LacZ expression in the dorsal midline. Open arrowheads indicate expression in scattered dorsal interneurons, potentially of dI1 subgroup. (M′ and N′) Insets are high magnifications of boxed regions of ependymal layers in (M) and (N), respectively.

(O) Quantification of Lmx1a-LacZ^{+} cells found in ependymal layers of control and dr^{J}/dr^{J} mutant spinal cord sections at P21. Representatively examples in (M) and (M′) and (N) and (N′). ****$p \leq 0.0001$. n = 3 mice for each. Error bars represent SEM.

Scale, 100 μm (A–F and M′–N′), 200 μm (G–N).

in control and dr^{6J}/dr^{6J} littermates at P0–P1 (Figures S4D′–S4K′). The distribution of excitatory and inhibitory neuronal populations appeared grossly undisrupted in the dr^{6J}/dr^{6J} mutant dorsal spinal cord, despite a size reduction of the lumbar segment for this specific mutant allele (dr^{J}/dr^{J} mice have normal spinal cord sizes) (Figure 5). In addition, we examined the central innervation of DRG primary afferents using IB4, CGRP, and VGLUT1 antibodies (Figures S5I–S5N) with adult control and dr^{6J}/dr^{6J} mutant lumbar sections. We found that DRG primary afferents innervated the proper spinal cord laminae with comparable signal

intensity (Figure S5U) between genotypes, suggesting that mutant spinal cords still retained enough integrity and appropriate axon guidance cues for the sensory central terminals to grow and innervate the right spinal cord layers.

Dreher Mutant Mice Display a Specific Deficit in RA Mechanoreceptor Ascending Axons

We next examined dorsal column development in the absence of RGLCs using the *dreher* mutant mice. Notably, within the DDC pathway, the volume of RET$^+$/NFH$^+$ and Parvalbumin (PV)-negative RA mechanoreceptive axons in the medial dorsal column was dramatically decreased in both dr^{6J}/dr^{6J} and dr^{J}/dr^{J} mutant mice compared to their control littermates (Figures 6A–6C and 6E–6G). This dorsal column phenotype became apparent by E15.5 by the time the dorsal column axons ascended in the dorsal funiculus (Figures S5Q and S5R), but not earlier at E13.5 when axons have not yet innervated the presumptive dorsal column (Figures S5O and S5P). In contrast, the volume of PV$^+$ proprioceptor axons, the shorter and more laterally located dorsal column axons, did not exhibit obvious differences in the both dr^{6J}/dr^{6J} and dr^{J}/dr^{J} mutants (Figures 6A, 6B, 6D–6F, and 6H). We did not observe any gross differences in the other dorsal column pathways, i.e. the CST (detected by PKCγ immunostaining) (Figures 6I–6J′) and PSDC pathways (genetically labeled in *Gsx1^{Cre}; Tau^{mGFP}* mice) (Figures 6K and 6L), between dr^{6J}/dr^{6J} mutants and control littermates (Figure 6M). Thus, the dorsal column deficit was exclusive to the RA mechanoreceptor axons of the DDC pathway.

To determine whether the reduction in RA mechanoreceptor volume under mutant conditions might be due to a developmental delay, we next examined dorsal column sections from adult control and mutant mice. Using semi-thin sections stained with toluidine blue to visualize axon cross-section profiles within the dorsal column, we found that the volume of the gracile fasciculus, which mainly contains the ascending axons of RA mechanoreceptors (Niu et al., 2013), was greatly reduced in mutant mice compared to controls (Figures 6N and 6O). High resolution images (Figures 6N′ and 6O′) showed that axon diameters were comparable between mutants and controls. However, the number of axons within the gracile fasciculus, quantified using a customized MATLAB program to automatically identify and count axon profiles (Niu et al., 2013), revealed a reduction of gracile fasciculus axon profiles by ~50% in the dr^{6J}/dr^{6J} mutant mice compared to controls (Figures 6P). These observations suggest a severe loss of RA mechanosensory ascending axons in *dreher* mutant mice that does not recover at later stages.

RA Mechanoreceptors in *Dreher* Mutants Are Generated Normally and Have No Intrinsic Deficits

Two possibilities can potentially explain the decreased volume of the gracile fasciculus and RA mechanoreceptor axon numbers in the *dreher* mutant dorsal column: (1) the *dreher* mutants experience perturbed neurogenesis or increased cell death of RA mechanoreceptors, or (2) the ascending axons of RA mechanoreceptors are shorter, resulting in fewer axon profiles within cross sections of the fascicles. To test the first possibility, we performed whole-mount DRG preparation and immunohistochemistry for RET$^+$ RA mechanoreceptors, which were identified as RET$^+$/NFH$^+$/PV$^-$ (Luo et al., 2009), and quantified their number from control and dr^{6J}/dr^{6J} mutants (Figures S6A and S6B). Both the absolute number of RA mechanoreceptors and the proportion of RA mechanoreceptors to all large diameter NFH$^+$ neurons were comparable between dr^{6J}/dr^{6J} mutants and control littermates (Figures S6C and S6D). This result indicates that both neurogenesis and survival of RA mechanoreceptors in the DRGs are largely unaffected in the dr^{6J}/dr^{6J} mutants.

To verify that any phenotypic deficit in axon length of RA mechanoreceptors was not due to a reduction in intrinsic growth ability, we dissociated DRG neurons from E14.5 control and mutant mouse embryos and grew the cells *in vitro* for 24 hr, to reach the equivalent of E15.5 developmental stage *in vivo*, at which time the dorsal column phenotype emerges in *dreher* mutants. We enriched RA mechanoreceptors in the dissociated DRG culture by adding only NRTN in the culture medium and identified mechanoreceptors in culture using RET and neurofilament medium chain (NFM) antibody co-staining (Figures S6E–S6F″). We then quantified computer tracings of the NFM$^+$ processes to evaluate the outgrowth of RA mechanoreceptors from both dr^{6J}/dr^{6J} and control littermates (Figures S6G and S6H) using three criteria: longest neurite length, total neurite outgrowth, and branching complexity. We found no significant differences in cultured RA mechanoreceptors from the mutants and the controls (Figures S6I–S6K). These results suggest that intrinsic growth capacity of RA mechanoreceptors is normal in *dreher* mutants.

Ascending Branches of Caudal RA Mechanoreceptors Are Dramatically Shortened in *Dreher* Mutant Mice

Given that the RA mechanoreceptor cell number and intrinsic growth ability were normal in dr^{6J}/dr^{6J} mutant mice, we hypothesized that the ascending axons of RA mechanoreceptors must be shorter due to an extrinsic deficit, most likely due to the lack of RGLCs. To test this idea, we took advantage of a sparse genetic labeling approach we previously developed (Niu et al., 2013), using a *Ret^{CreERT2}; Rosa26^{iAP}* allele and alkaline phosphatase color reaction to visualize individual RA mechanoreceptors in whole mount spinal cord. Consistent with what was previously described, nearly all RA mechanoreceptor ascending axons from each spinal level reached the medulla under normal conditions. In contrast, under mutant conditions the ascending axons of many RA mechanoreceptors terminated prematurely within the dorsal column. A representative example (Figure 7A) shows one mechanoreceptor axon originating from a lumbar (L) 4 DRG, which bifurcates upon entry into the dorsal horn and gives rise to normal third order collaterals as it projects along the lateral dorsal spinal cord (Figure 7B). In this example, the ascending axon projects rostrally, but stops prematurely at thoracic (T) 7 (Figure 7C). In total, we quantified the central projections of AP-labeled RA mechanoreceptors from 12 *dr^{6J}/dr^{6J}; Ret^{CreERT2}; Rosa26^{iAP}* mutants (84 neurons total) and 10 control animals (60 neurons total). Approximately half of the ascending RA mechanoreceptive axons in the dr^{6J}/dr^{6J} mutants failed to reach the medulla by 3 weeks of age (Figure 7D, 7E, and 7G). This deficit was especially prominent in axons originating from DRGs at sacral, lumbar, and caudal thoracic levels below T7 (Figure 7F). In contrast, the descending axons of the traced RA mechanoreceptors and the third-order collaterals innervating

OPEN
ACCESS
CellPress

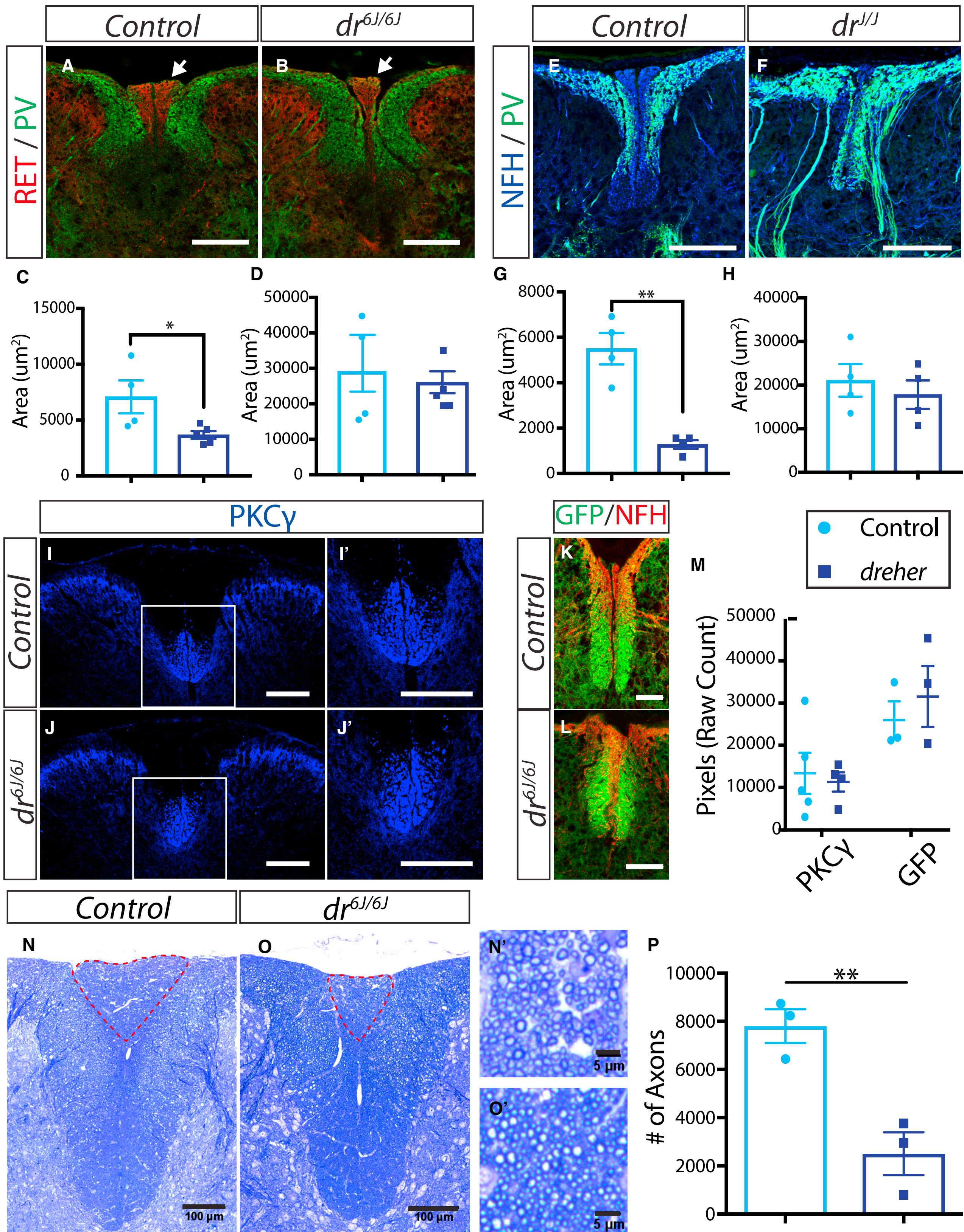

(legend on next page)

the dorsal spinal cord showed no significant deficit in the dr^{6J}/dr^{6J} mutants (Figures 7H, S5I–S5N, and S5U). These results reveal that growth of the longest projecting dorsal column axons (i.e., axons from the caudal RA mechanoreceptors) is specifically affected in dr^{6J}/dr^{6J} mutant mice, while other shorter axon branches of those same neurons are not affected. Given that the intrinsic growth capacity of RA mechanoreceptors is largely normal in the dr^{6J}/dr^{6J} mutant mice (Figures S6E–S6K), our findings indicate that the loss of RGLCs in *dreher* mutant mice leads to a non-cell autonomous environmental deficiency that is critical for the growth and/or maintenance of extra-long spinal cord longitudinal axons.

DISCUSSION

Spinal cord longitudinal axons convey critical sensory and motor information over great distances through the body, but little is known about the molecular and cellular mechanisms that allow them to extend and establish these connections during development. In this study, we identified a cellular structure formed by the roof plate-derived RGLCs. These cells express a variety of growth-supportive factors and form a network of processes closely contacting the longest developing axons within the spinal cord dorsal column. We showed that the RGLCs are required for normal long-distance growth/maintenance of these axons *in vivo*. Thus, we propose a model in which RGLCs form a necessary "highway" of processes to provide critical molecular and mechanical support for extra-long spinal cord longitudinal axons (Figures S7B–S7E).

Identification and Characterization of Dorsal Midline RGLCs

During early development of the spinal cord prior to E13.5, the roof plate functions both as a source of neural progenitors and as a dorsalizing signaling center (Lee and Jessell, 1999). Roof plate ablation through different genetic approaches indicates that this structure is required for neurogenesis and specification of subsets of some dorsal spinal cord interneurons (Lee et al., 2000; Millen et al., 2004) (Figure S7A). However, the fate of roof plate-derived cells after E13.5, and whether there remains a role for them in later stages of spinal cord development, is largely unclear. By genetically tracing roof plate cells using $Lmx1a^{Cre}$ mice, we show here that roof plate-lineage cells remaining in the dorsal midline of the spinal cord migrate toward the central canal around E14.5 and become RGLCs (Figure S7A) during the developmental growth phase of adjacent ascending dorsal column axons (Figure 4). The apical processes of the RGLCs form a network and express a number of candidate growth factors to which RA mechanoreceptors are responsive *in vitro* (Figures S2 and S3). As discussed below, we believe that these cells play critical developmental roles in promoting longitudinal axon growth/maintenance in a non-autonomous manner from E14.5 to neonatal (Figures S7B–S7E). They persist in the dorsal spinal cord midline to form the dorsal median sulcus postnatally (Figures S2H–S2I′).

Function of RGLCs in Supporting Long Distance Axonal Growth Is Independent from Early Developmental Roles of the Roof Plate

The roof plate plays an important role in early spinal cord development (Augsburger et al., 1999; Chizhikov and Millen, 2004; Lee et al., 2000; Liem et al., 1997; Millen et al., 2004). While *dreher* mutant mice display roof plate deficits (Chizhikov and Millen, 2005; Millonig et al., 2000), the mutants still express some *Bmp* signaling pathway markers (*Msx1/2* and *Wnt*), indicating that signaling activity is not fully abolished (Millen et al., 2004). This residual signaling, combined with existing ectodermal signaling (Dickinson et al., 1995; Liem et al., 1997; Liem et al., 1995), may lead to less severe developmental deficits of *dreher* mutant spinal cord than the roof plate complete ablation models. Indeed, we found that expression of mature interneuron markers is grossly normal in the *dreher* mutants, and that some dI1 neuronal genesis/migration still occurs, as shown using genetic tracing at developmental and postnatal stages (Figures 5 and S4). In addition, other dorsal interneuron precursor types, such as dI2, dI3, dILA, and dILB, were generated normally in number in the *dreher* mutants (Figure S5). Moreover, different types of central terminals of primary sensory neurons grow and innervate the right dorsal spinal cord layers (Figure S5). Thus, despite the known early developmental deficits of roof plate lesion, the *dreher* mutant dorsal spinal cord neurons seem to retain sufficient integrity and appropriate environmental cues for growth and innervation of sensory axonal collaterals.

Previous observations also showed that neural crest cells, which share a common precursor with roof plate cells (Echelard

Figure 6. The Gracile Fasciculus Size Is Reduced in *dreher* Mutants

(A and B) Co-staining of RET and PV, respective markers for mechanoreceptors (white arrows) and proprioceptors, in controls (A) and $dr^{6J/6J}$ mutants (B) cervical spinal cord sections at P7–P8.

(C and D) Quantification of gracile region containing PV-negative mechanoreceptors (C), and cuneate area containing PV-positive proprioceptors (D). $^{*}p \leq 0.05$.

(E and F) Co-staining of PV and NFH to show proprioceptors and dorsal column axons, respectively, in controls (E) and dr^{J}/dr^{J} mutants (F) thoracic spinal cord sections at P7–P8.

(G and H) Quantification of gracile region containing PV-negative mechanoreceptors (G), and cuneate area containing PV-positive proprioceptors (H). $^{**}p \leq 0.01$.

(I–J′) PKCγ staining of 6-week-old cervical spinal cord sections in control (I and I′) and dr^{6J}/dr^{6J} mutant mice (J and J′). (I′) and (J′) are magnified views of boxed regions of (I) and (J).

(K and L) Co-staining of lumbar spinal cord sections with antibodies against GFP and NFH in control (K) and dr^{6J}/dr^{6J} (L) mice at P0. PSDC neurons and axons are genetically labeled with $Gsx1^{Cre}$; Tau^{mGFP} reporter.

(M) Quantification of raw pixel count above background levels.

(N–O′) Semi-thin cervical spinal cord sections with toluidine blue staining of controls (N) and $dr^{6J/6J}$ mutants (O) at adult (5–6 weeks) stages. Gracile fasciculi are outlined with dotted red lines. (N′ and O′) High magnification of (N) and (O) gracile fasciculi axons.

(P) Quantification of axon number within gracile fasciculi of controls and $dr^{6J/6J}$ mutants. $^{**}p \leq 0.01$.

(C–H, M, and P) Error bars represent SEM. Scale, 100 μm (A, B, I–J′, N, and O), 50 μm (K and L), 5 μm (N′ and O′). n = 3 mice for each.

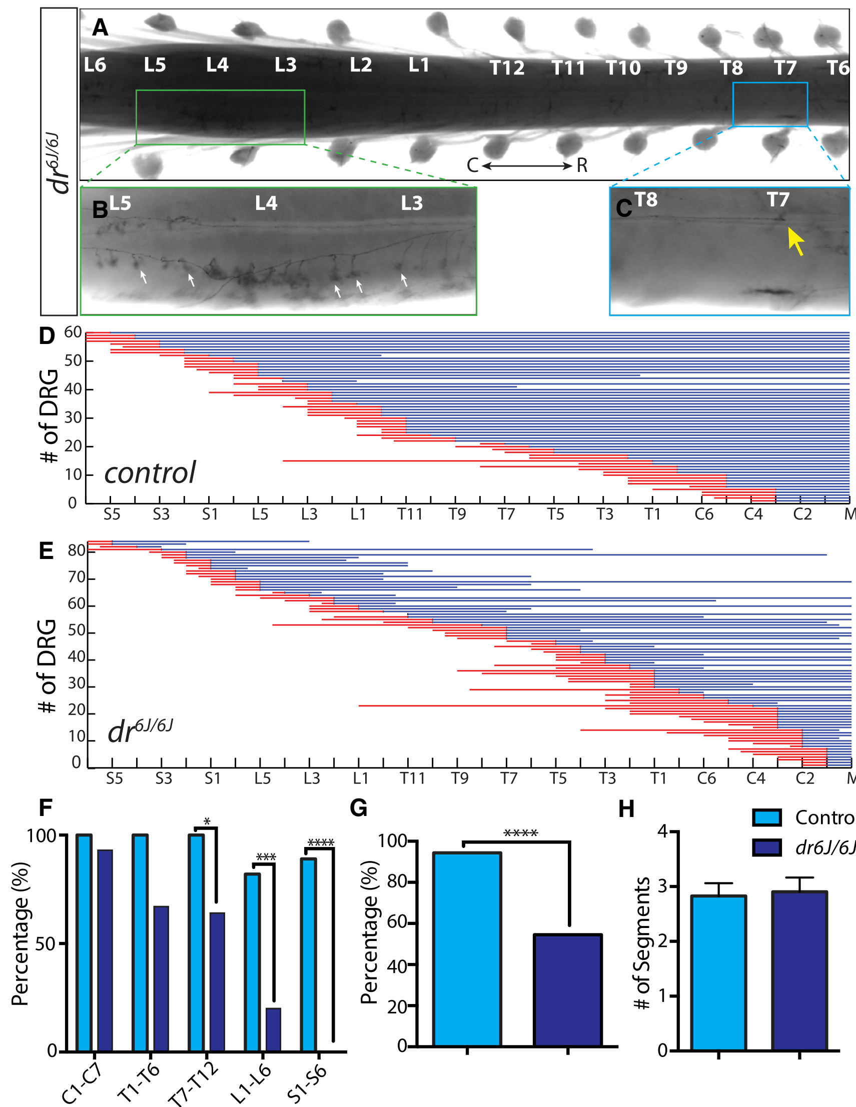

Figure 7. Aberrantly Short Ascending Axon Branches from Caudal RA Mechanoreceptors in *dreher* Mutant Mice

(A–C) Representative example of P21 dr^{6J}/dr^{6J} whole mount spinal cord with sparsely labeled mechanoreceptors using $Ret^{CreERT2}$; $Rosa26^{iAP}$ reporter (A). Higher magnification shows the central projection of one L4 DRG with normal third order collateral branches (white arrows) innervating the dorsal spinal cord (B) and premature termination of ascending axon at T7 (C) (yellow arrow).

(D and E) Representation of sparsely labeled ascending (blue lines) and descending (red lines) mechanoreceptive axons in control (D) and dr^{6J}/dr^{6J} mutant (E) mice. x axis denotes vertebral level, and y axis denotes individual mechanoreceptor neurons.

(F) Quantification of ascending mechanoreceptor axons reaching the medulla in control and mutant mice according to vertebral level of innervation (x axis).

(G) Total number of ascending mechanoreceptor axons innervating the medulla in controls and mutant mice.

(H) Number of vertebral segments crossed by descending mechanoreceptor axons in controls and dr^{6J}/dr^{6J} mutant mice. *p $\leq$ 0.05; ***p $\leq$ 0.001; ****p $\leq$ 0.0001. n = 12 mice for dr^{6J}/dr^{6J} mutant mice and n = 10 mice for littermate control. Error bars represent SEM.

et al., 1994), and their progeny (e.g., DRG neurons) are normal in *dreher* mutant mice (Chizhikov and Millen, 2004; Lee et al., 2000). Consistently, we found that the number and intrinsic growth ability of RA mechanoreceptors were largely unaffected (Figure S6). Finally, the exclusivity of the phenotype to just the ascending axon branch of the caudal RA mechanoreceptors in *dreher* mutant mice (Figures 6 and 7) argues against significant nonspecific secondary effects. Any existing secondary effects from early dorsal spinal cord developmental deficits in the mutants would likely result in deficiencies in all dorsal column axons, rather than one axon branch of a single neuron population. In particular, secondary effects would likely heavily impact proprioceptors, which form direct synapses with dI1 interneurons under normal conditions, or PSDC neurons, whose cell bodies are within the dorsal spinal cord. However, both proprioceptive and PSDC axons in the dorsal column are largely normal in *dreher* mutant mice (Figure 6). Taken all into consideration, we strongly believe that the roof plate's function in early dorsal spinal cord development, and its later function as RGLCs in promoting growth/maintenance of RA mechanoreceptor axons in the dorsal column, are likely two independent processes (Figure S7A).

Absence of RGLCs Specifically Affects Ascending Branches of Caudal RA Mechanoreceptor Axons

The mouse dorsal column, which contains two groups of ascending axons, the DDC and PSDC, and one group of descending axons, the CST, provides a unique model to examine developmental mechanisms underlying long distance growth of different neuronal types. Here, we showed that disruption of RGLCs specifically impairs the growth of ascending axons of the most caudal RA mechanoreceptors, but not the ascending axons of proprioceptors and PSDC neurons (Figures 6 and 7). Furthermore, we did not observe any gross impairment in the development of the descending CST axons in the absence of RGLCs (Figures 6I–6J′ and 6M). Given the non-overlapping developmental time windows between the ascending and descending pathways, our results support the idea that the two pathways rely on distinct developmental mechanisms. Additionally, we found that the RGLCs appear to undergo a fate change postnatally, as suggested by their downregulation of ZIC2 (Figures 3C–3C′), indicating that CST axons likely do not require RGLCs for their normal development. In contrast, PSDC and PV^{+} proprioceptive axons grow into the dorsal column simultaneously with RA mechanoreceptors (Figures 1C–1F), but their development

also appears largely normal in *dreher* mutant mice (Figures 6A–6H and 6K–6M). Based on single cell tracing of RA mechanoreceptors and proprioceptors (Niu et al., 2013), we know that the ascending axons of RA mechanoreceptors from all vertebral levels project through the entire spinal cord to innervate the dorsal column nuclei in the brain stem, whereas proprioceptors have much shorter axons (~6 to 7 spinal cord segments on average) (Niu et al., 2013), with caudal proprioceptors (~T7 and below) terminating within the spinal cord dorsal column and synapsing with Clarke's column. Thus, the long-distance projecting RA mechanoreceptors of the DDC pathway might require more support than the shorter projecting proprioceptors. In addition, despite the dramatic phenotype of their ascending branches, other aspects of RA mechanoreceptor central axon branch elaboration and pathfinding are largely normal in the *dreher* mutants: their central projections enter the dorsal column normally, their branches navigate in the correct directions along the spinal cord axis, they give rise to a normal volume of third-order collaterals, and their descending axons grow normal lengths (Figure 7H). In contrast, *Ret* mutant mice, which have a dramatic deficit in RA mechanoreceptor survival, growth of third-order collaterals, and formation of peripheral end organs (Fleming et al., 2015, 2016; Luo et al., 2009), have a relatively normal dorsal column at P0 (data not shown). Therefore, separate mechanisms and signaling pathways must be required for the development of different axon branches of RA mechanoreceptors. Taken together, our results support a model in which RGLCs are not required for basal growth of DRG and spinal cord axons, but instead provide a specialized mechanism for the promotion and/or maintenance of extra long-distance growth of RA mechanoreceptor ascending axons to span the entire spinal cord (Figures S7B–S7E).

Lastly, radial glial cells have been shown to play a variety of important developmental functions, including the generation of neural progenitors and providing structural support for migrating newly born neurons (Rakic, 1971). They were also proposed to provide a permissive growth-conducive environment for axon bundles during both development and regeneration in regenerative species, such as fish or newt (the "blue print" hypothesis) (Schwab and Schnell, 1991; Singer et al., 1979). However, despite interesting correlative observations, direct evidence to show roles for radial glial cells in promoting long-distance axon growth is lacking, especially in the mammalian system. In this study, we found that roof plate-derived dorsal column midline cells express a number of radial glial-specific markers, as shown by both our RNA sequencing and immunohistochemistry, and have radial glial-like morphology (Figures 2E, 2F, 4, and 5). In addition, their radial processes form a network perpendicular to the growing dorsal column axons, which is required specifically for the lengthy growth of RA mechanoreceptive longitudinal axons (Figure 7B–7E). Thus, our study provides direct evidence that radial glial cells form an important scaffold to guide, support, or maintain long-distance axon growth during development. Because these cells remain *in situ* postnatally after undergoing fate changes, RGLCs could provide potential targets for future studies to revert them to an embryonic growth-promoting state as a therapeutic approach to encourage mammalian spinal cord axon regeneration post-injury.

EXPERIMENTAL PROCEDURES

Animals

Mice were housed in a barrier facility in the Hill Pavilion, University of Pennsylvania and vivaria at the University of Chicago, Seattle Children's Research Institute and the University of Tennessee Health Sciences Center. All procedures were conducted according to animal protocols approved by Institutional Animal Care and Use Committees of the respective institutions and the National Institutes of Health guidelines. Mice used in this paper were described previously: $Ret^{CreERT2}$, Ret^{CFP}, $Rosa26^{Tdt}$ (JAX stock #007908), $Rosa26^{ZsGreen}$ (JAX stock #007906), $Rosa26^{iAP}$ (JAX stock #003309), $Rosa26^{LacZ}$ (JAX stock #003309), Tau^{mGFP} (JAX stock #021162), $Gsx1^{Cre}$, *dreher* (dr^{6J} and dr^{J}), $Lmx1a^{Cre}$ (Chizhikov et al., 2006; Cui et al., 2016; Luo et al., 2009; Millonig et al., 2000). Both sexes were used for all experiments, from the ages of E10.5 through adult (ages detailed in figure legend). Timed-pregnancy female Sprague-Dawley rats (strain code 400) were ordered from Charles River and sacrificed for DRG dissociation at E16. This procedure was approved by IACUC of Temple University.

Image Acquisition and Quantification

Fluorescent images were captured using a Leica SP5II confocal microscope or a Zeiss AxioImager A2 microscope. Bright field images were taken using Leica DM5000B microscope, and semi-thin sections were imaged on the DM5000B with a motor stage and power-mosaic mode. For quantifying the central projection defects of mechanoreceptors of dr^{6J} and control mice, whole-mount AP coloring spinal cord was imaged with a Leica M205C dissection microscope, the ascending and descending information of sparsely labeled cells was summarized and represented in bar graphs using a program written in MATLAB (The MathWorks). Approximately 8–10 sections of spinal cord/DRG or 5–10 whole-mount DRGs per animal and three mice per genotype were used for quantification and statistical analysis of immunostainings. Quantification of dI2-3 and dILA/dILB interneurons was performed on 12-μm thick cryosections (3 sections per embryo, 3 embryos per genotype). Quantification of axons from semi-thin sections was performed using a program for MATLAB based on axon diameter cutoffs (Niu et al., 2013). Cell number counting was performed using ImageJ, while column graphs and scatterplots were generated in GraphPad Prism 5. Pearson's chi-square test and unpaired Student's t test were performed accordingly. All error bars are ±SEM.

Other Experimental Procedures

See the Supplemental Experimental Procedures.

DATA AND SOFTWARE AVAILABILITY

The accession number for the RNA sequencing data set reported in this paper is Mendeley Data (https://data.mendeley.com/datasets/j79mscjcw8/1). It can also be found at GEO with accession number GSE114193.

SUPPLEMENTAL INFORMATION

Supplemental Information includes Supplemental Experimental Procedure and seven figures and can be found with this article online at https://doi.org/10.1016/j.celrep.2018.05.025.

ACKNOWLEDGMENTS

We thank members of the Luo lab for helpful comments on the manuscript. We thank the UPenn Penn Genomic Analysis Core (PGAC) for conducting the RNA sequencing, and T. Perlmann, Karolinska Institute, Stockholm, Sweden for Lmx1b antibody. This work was supported by the NIH (1R01NS083702 and R01NS094224 to W.L., R01NS080390 to K.J.M., R01 NS093009 to V.V.C., and F31-NS100325-01A1 and T32GM07517 to K.K.), and the Klingenstein-Simons Fellowship Awards in the Neurosciences to W.L.

AUTHOR CONTRIBUTIONS

K.K. and J.N. performed most of the experiments and data analysis. W.L. mapped the *dr*$^{6J/6J}$ mutant allele. Z.W. performed the data analysis of RNA-seq. P.H. generated the tissue of *Lmx1a*^{cre}*; Rosa*^{Tdt} and *dr*^{J} mice. L.D. wrote the code for MATLAB program. A.L. performed genetic tracing of *dreher* mutant mice. J.N., K.K., G.T., V.V.C., K.M., and W.L. designed the experiments and wrote the manuscript. All authors revised the paper and contributed conceptually.

DECLARATION OF INTERESTS

The authors declare no competing interests.

Received: June 2, 2017
Revised: March 2, 2018
Accepted: May 3, 2018
Published: June 5, 2018

REFERENCES

Augsburger, A., Schuchardt, A., Hoskins, S., Dodd, J., and Butler, S. (1999). BMPs as mediators of roof plate repulsion of commissural neurons. Neuron *24*, 127–141.

Bergstrom, D.E., Gagnon, L.H., and Eicher, E.M. (1999). Genetic and physical mapping of the dreher locus on mouse chromosome 1. Genomics *59*, 291–299.

Bourikas, D., Pekarik, V., Baeriswyl, T., Grunditz, A., Sadhu, R., Nardó, M., and Stoeckli, E.T. (2005). Sonic hedgehog guides commissural axons along the longitudinal axis of the spinal cord. Nat. Neurosci. *8*, 297–304.

Chizhikov, V.V., and Millen, K.J. (2004). Control of roof plate formation by Lmx1a in the developing spinal cord. Development *131*, 2693–2705.

Chizhikov, V.V., and Millen, K.J. (2005). Roof plate-dependent patterning of the vertebrate dorsal central nervous system. Dev. Biol. *277*, 287–295.

Chizhikov, V., Steshina, E., Roberts, R., Ilkin, Y., Washburn, L., and Millen, K.J. (2006). Molecular definition of an allelic series of mutations disrupting the mouse Lmx1a (dreher) gene. Mamm. Genome *17*, 1025–1032.

Chizhikov, V.V., Lindgren, A.G., Mishima, Y., Roberts, R.W., Aldinger, K.A., Miesegaes, G.R., Currle, D.S., Monuki, E.S., and Millen, K.J. (2010). Lmx1a regulates fates and location of cells originating from the cerebellar rhombic lip and telencephalic cortical hem. Proc. Natl. Acad. Sci. USA *107*, 10725–10730.

Cui, L., Miao, X., Liang, L., Abdus-Saboor, I., Olson, W., Fleming, M.S., Ma, M., Tao, Y.X., and Luo, W. (2016). Identification of early RET + deep dorsal spinal cord interneurons in gating pain. Neuron *91*, 1137–1153.

Dickinson, M.E., Selleck, M.A., McMahon, A.P., and Bronner-Fraser, M. (1995). Dorsalization of the neural tube by the non-neural ectoderm. Development *121*, 2099–2106.

Echelard, Y., Vassileva, G., and McMahon, A.P. (1994). Cis-acting regulatory sequences governing Wnt-1 expression in the developing mouse CNS. Development *120*, 2213–2224.

Escalante, A., Murillo, B., Morenilla-Palao, C., Klar, A., and Herrera, E. (2013). Zic2-dependent axon midline avoidance controls the formation of major ipsilateral tracts in the CNS. Neuron *80*, 1392–1406.

Fleming, M.S., Vysochan, A., Paixão, S., Niu, J., Klein, R., Savitt, J.M., and Luo, W. (2015). Cis and trans RET signaling control the survival and central projection growth of rapidly adapting mechanoreceptors. eLife *4*, e06828.

Fleming, M.S., Li, J.J., Ramos, D., Li, T., Talmage, D.A., Abe, S.-I., Arber, S., and Luo, W. (2016). A RET-ER81-NRG1 signaling pathway drives the development of Pacinian corpuscles. J. Neurosci. *36*, 10337–10355.

Helms, A.W., and Johnson, J.E. (2003). Specification of dorsal spinal cord interneurons. Curr. Opin. Neurobiol. *13*, 42–49.

Lee, K.J., and Jessell, T.M. (1999). The specification of dorsal cell fates in the vertebrate central nervous system. Annu. Rev. Neurosci. *22*, 261–294.

Lee, K.J., Dietrich, P., and Jessell, T.M. (2000). Genetic ablation reveals that the roof plate is essential for dorsal interneuron specification. Nature *403*, 734–740.

Liem, K.F., Jr., Tremml, G., Roelink, H., and Jessell, T.M. (1995). Dorsal differentiation of neural plate cells induced by BMP-mediated signals from epidermal ectoderm. Cell *82*, 969–979.

Liem, K.F., Jr., Tremml, G., and Jessell, T.M. (1997). A role for the roof plate and its resident TGFbeta-related proteins in neuronal patterning in the dorsal spinal cord. Cell *91*, 127–138.

Liu, Y., Shi, J., Lu, C.-C.C., Wang, Z.-B.B., Lyuksyutova, A.I., Song, X.-J.J., and Zou, Y. (2005). Ryk-mediated Wnt repulsion regulates posterior-directed growth of corticospinal tract. Nat. Neurosci. *8*, 1151–1159.

Luo, W., Enomoto, H., Rice, F.L., Milbrandt, J., and Ginty, D.D. (2009). Molecular identification of rapidly adapting mechanoreceptors and their developmental dependence on ret signaling. Neuron *64*, 841–856.

Lyuksyutova, A.I., Lu, C.-C.C., Milanesio, N., King, L.A., Guo, N., Wang, Y., Nathans, J., Tessier-Lavigne, M., and Zou, Y. (2003). Anterior-posterior guidance of commissural axons by Wnt-frizzled signaling. Science *302*, 1984–1988.

Millen, K.J., Millonig, J.H., and Hatten, M.E. (2004). Roof plate and dorsal spinal cord dl1 interneuron development in the dreher mutant mouse. Dev. Biol. *270*, 382–392.

Millonig, J.H., Millen, K.J., and Hatten, M.E. (2000). The mouse Dreher gene Lmx1a controls formation of the roof plate in the vertebrate CNS. Nature *403*, 764–769.

Mizuguchi, R., Kriks, S., Cordes, R., Gossler, A., Ma, Q., and Goulding, M. (2006). Ascl1 and Gsh1/2 control inhibitory and excitatory cell fate in spinal sensory interneurons. Nat. Neurosci. *9*, 770–778.

Niu, J., Ding, L., Li, J.J., Kim, H., Liu, J., Li, H., Moberly, A., Badea, T.C., Duncan, I.D., Son, Y.-J., et al. (2013). Modality-based organization of ascending somatosensory axons in the direct dorsal column pathway. J. Neurosci. *33*, 17691–17709.

Paixão, S., Balijepalli, A., Serradj, N., Niu, J., Luo, W., Martin, J.H., and Klein, R. (2013). EphrinB3/EphA4-mediated guidance of ascending and descending spinal tracts. Neuron *80*, 1407–1420.

Rakic, P. (1971). Guidance of neurons migrating to the fetal monkey neocortex. Brain Res. *33*, 471–476.

Schwab, M.E., and Schnell, L. (1991). Channeling of developing rat corticospinal tract axons by myelin-associated neurite growth inhibitors. J. Neurosci. *11*, 709–721.

Singer, M., Nordlander, R.H., and Egar, M. (1979). Axonal guidance during embryogenesis and regeneration in the spinal cord of the newt: the blueprint hypothesis of neuronal pathway patterning. J. Comp. Neurol. *185*, 1–21.

Wessels, W.J., Feirabend, H.K., and Marani, E. (1991). Development of projections of primary afferent fibers from the hindlimb to the gracile nucleus: a WGA-HRP study in the rat. Brain Res. Dev. Brain Res. *63*, 265–279.

Yam, P.T., Kent, C.B., Morin, S., Farmer, W.T., Alchini, R., Lepelletier, L., Colman, D.R., Tessier-Lavigne, M., Fournier, A.E., and Charron, F. (2012). 14-3-3 proteins regulate a cell-intrinsic switch from sonic hedgehog-mediated commissural axon attraction to repulsion after midline crossing. Neuron *76*, 735–749.

Yuengert, R., Hori, K., Kibodeaux, E.E., McClellan, J.X., Morales, J.E., Huang, T.P., Neul, J.L., and Lai, H.C. (2015). Origin of a non-Clarke's column division of the dorsal spinocerebellar tract and the role of caudal proprioceptive neurons in motor function. Cell Rep. *13*, 1258–1271.